The Journal of Chemical Physics

Ab initio intermolecular potential energy surface for the CO_2—N_2 system and related thermophysical properties

Cite as: J. Chem. Phys. **148**, 214306 (2018); https://doi.org/10.1063/1.5034347
Submitted: 10 April 2018 . Accepted: 17 May 2018 . Published Online: 07 June 2018

Johann-Philipp Crusius, Robert Hellmann, Juan Carlos Castro-Palacio, and Velisa Vesovic

Ab initio intermolecular potential energy surface for the CO_2—N_2 system and related thermophysical properties

Johann-Philipp Crusius,[1] Robert Hellmann,[2,a)] Juan Carlos Castro-Palacio,[1] and Velisa Vesovic[1]
[1]*Department of Earth Science and Engineering, Imperial College London, London SW7 2AZ, United Kingdom*
[2]*Institut für Chemie, Universität Rostock, 18059 Rostock, Germany*

(Received 10 April 2018; accepted 17 May 2018; published online 7 June 2018)

A four-dimensional potential energy surface (PES) for the interaction between a rigid carbon dioxide molecule and a rigid nitrogen molecule was constructed based on quantum-chemical *ab initio* calculations up to the coupled-cluster level with single, double, and perturbative triple excitations. Interaction energies for a total of 1893 points on the PES were calculated using the counterpoise-corrected supermolecular approach and basis sets of up to quintuple-zeta quality with bond functions. The interaction energies were extrapolated to the complete basis set limit, and an analytical site–site potential function with seven sites for carbon dioxide and five sites for nitrogen was fitted to the interaction energies. The CO_2—N_2 cross second virial coefficient as well as the dilute gas shear viscosity, thermal conductivity, and binary diffusion coefficient of CO_2—N_2 mixtures were calculated for temperatures up to 2000 K to validate the PES and to provide reliable reference values for these important properties. The calculated values are in very good agreement with the best experimental data. *Published by AIP Publishing.* https://doi.org/10.1063/1.5034347

I. INTRODUCTION

Thermophysical properties of low-density gases are exclusively determined by binary interactions and are thus directly connected to the intermolecular pair potential energy surfaces (PESs). Knowledge of the pair potentials enables the calculation of values for the second virial coefficient and transport properties in the dilute gas limit by means of statistical-mechanical relations and the kinetic theory of gases, respectively. Accurate pair PESs for small molecules, for instance, methane,[1] water,[2] hydrogen,[3] hydrogen sulfide,[4] nitrogen,[5] carbon dioxide,[6] ethylene oxide,[7] ethane,[8] and propane,[9] can be routinely constructed these days using high-level quantum-chemical *ab initio* methods to determine the binary interaction energies.

Recently, Hellmann and co-workers have extended their work on pure gases[1,4–13] to binary mixtures, namely, CH_4—N_2,[14,15] CH_4—CO_2,[16] CH_4—H_2S,[16] H_2S—CO_2,[16] CH_4—C_3H_8,[17] and CO_2—C_3H_8,[17] and successfully validated the respective kinetic theory expressions for the transport properties.[14–16] The extension of the calculations to binary mixtures provides not only accurate thermophysical property data for such systems but also all the input data for the calculation of thermophysical properties of any multicomponent mixture consisting of species for which the binary properties are available. The addition of the CO_2—N_2 system will allow for a better characterization of thermophysical properties of a number of industrially important gas mixtures, in particular, for (i) flue gas and process streams used in capturing and cleaning of CO_2 before injection into reservoirs as part of the carbon capture and storage (CCS) process; (ii) natural gas, where the recent discoveries of CO_2-rich reservoirs with non-negligible amounts of N_2 require updating and extending the existing thermophysical data; and (iii) combustion modeling. Furthermore, thermophysical data for both species and their mixtures are needed for modeling of Earth's and other planets' atmospheres.

To determine properties of low-density CO_2—N_2 gas mixtures, pair potentials for all three distinct binary interactions are required, i.e., CO_2—CO_2, N_2—N_2, and the unlike interaction CO_2—N_2. Hellmann has already published accurate pair potentials for the pure components.[5,6] Hence, only a CO_2—N_2 potential of similar quality needed to be developed. A literature search indicated that in 2015 Nasri *et al.*[18] developed a CO_2—N_2 pair potential of comparable quality; however, their paper does not provide the details necessary to reproduce the PES, and the attempts by the present authors to obtain these details were unsuccessful.

We have therefore developed a new CO_2—N_2 pair potential in this paper. It is based on a total of 1893 points on the PES for which *ab initio* calculations up to the coupled-cluster level with single, double, and perturbative triple excitations [CCSD(T)][19] have been performed using the supermolecular approach.[20] An analytical site–site potential with seven and five sites for CO_2 and N_2, respectively, has been fitted to the computed interaction energies. Calculation of the cross second virial coefficient for CO_2—N_2 and, in conjunction with the two pure-species pair potentials, transport properties of dilute CO_2—N_2 gas mixtures served to validate the new PES and to provide valuable reference data for these properties.

a)Electronic mail: robert.hellmann@uni-rostock.de

Section II details the *ab initio* calculations for the CO_2—N_2 molecule pair and the development of the analytical potential function. In Sec. III, we discuss the cross second virial coefficient and compare with experimental data. Section IV contains the results of the transport property calculations and a comparison with data from the literature. A summary and conclusions are given in Sec. V.

II. INTERMOLECULAR POTENTIAL

A. *Ab initio* calculations

The CO_2 and N_2 molecules were treated as rigid rotors in all *ab initio* calculations. To maintain consistency with the pair potentials for CO_2—CO_2[6] and N_2—N_2,[5] we used the same bond lengths, i.e., a C—O bond length of 1.1625 Å and an N—N bond length of 1.1014 Å in all quantum-chemical calculations. These bond length values reflect the zero-point vibrationally averaged geometries. The configurations of the two rigid molecules are described as a function of the center-of-mass distance R between molecule 1 (CO_2) and molecule 2 (N_2) and the three angles θ_1, θ_2, and ϕ as illustrated in Fig. 1(a); see also the supplementary material.

A total of 93 distinct angular configurations and up to 22 center-of-mass separations between 1.75 Å and 10.0 Å were considered. Of the resulting 2046 (93 × 22) points, 155 were discarded because of a strong overlap of the molecules at small distances or failing quantum-chemical calculations for points in the strongly repulsive region of the PES due to near-linear dependencies in the basis sets. The interaction energies $V(R, \theta_1, \theta_2, \phi)$ were determined following the supermolecular approach accounting for the full counterpoise correction[20] at the frozen-core resolution of identity Møller-Plesset perturbation theory of second order (RI-MP2)[21,22] level of theory. The RI-JK approximation[23,24] was used for the Hartree–Fock (HF) part. For the calculations, we employed the aug-cc-pVXZ[25] basis sets with $X = 4$ (Q) and $X = 5$ together with the auxiliary basis sets aug-cc-pV5Z-JKFIT[26] and aug-cc-pV5Z-MP2FIT[27] for both basis set levels. Additionally, bond functions have been placed midway along the R axis of each configuration. Following Patkowski,[28] these bond functions are the hydrogenic functions of the respective basis set and auxiliary basis set levels as for the other atoms. The results for the interaction energies using the RI-MP2 method differ negligibly from those obtained using the standard MP2 approach as we have checked for selected configurations, while the RI-MP2 method is significantly faster. The correlation parts of the interaction energies, $V_{\text{RI-MP2 corr}}$, were extrapolated to the complete basis set (CBS) limit using the well-established two-point scheme recommended by Halkier *et al.*,[29]

$$V_{\text{RI-MP2 corr}}(X) = V^{\text{CBS}}_{\text{RI-MP2 corr}} + \alpha X^{-3}. \tag{1}$$

The HF contributions, on the other hand, were taken from the $X = 5$ basis set level where they are effectively converged. Furthermore, we performed counterpoise-corrected supermolecular calculations at the frozen-core CCSD(T)/aug-cc-pVTZ and CCSD(T)/aug-cc-pVQZ levels of theory for all points on the PES to increase the accuracy of the interaction energies. The differences between the CCSD(T) and MP2 interaction energies [the latter being a byproduct of the CCSD(T) calculations] were extrapolated to the CBS limit in an analogous manner as the $V_{\text{RI-MP2 corr}}$ values and added to the RI-MP2/CBS interaction energies, thereby obtaining a very good approximation for the frozen-core CCSD(T)/CBS level. The coupled-cluster calculations have been performed without any bond functions because test calculations have shown that this results in a better convergence of the extrapolated CBS energies. The results of the *ab initio* calculations for all points on the PES are given in the supplementary material. All RI-MP2 and CCSD(T) calculations were carried out using ORCA 3.0.3[30] and CFOUR,[31] respectively.

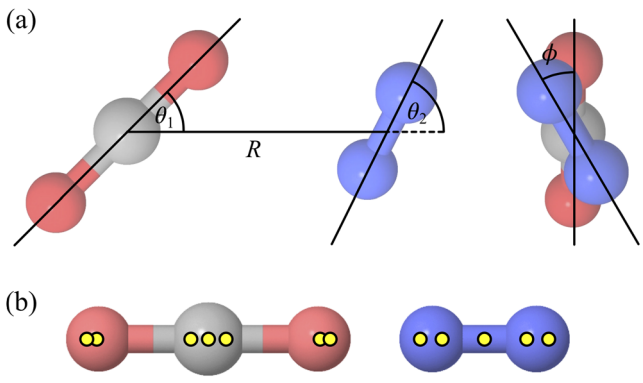

FIG. 1. (a) Internal coordinates of the CO_2—N_2 system. (b) Visualization of the positions of the interaction sites in each molecule used for the analytical potential function.

B. Analytical potential function

A site–site potential function with seven sites for CO_2 and five sites for N_2 was fitted to the final CCSD(T)/CBS interaction energies. Each isotropic site–site interaction is given by

$$V_{ij}(R_{ij}) = A_{ij} \exp(-\alpha_{ij} R_{ij}) - f_6(b_{ij}, R_{ij}) \frac{C_{6\,ij}}{R_{ij}^6} + \frac{q_i q_j}{R_{ij}}, \tag{2}$$

where R_{ij} is the distance between site i in the CO_2 molecule and site j in the N_2 molecule. The damping function f_6 is given as[32]

$$f_6(b_{ij}, R_{ij}) = 1 - \exp(-b_{ij} R_{ij}) \sum_{k=0}^{6} \frac{(b_{ij} R_{ij})^k}{k!}. \tag{3}$$

The total potential is then obtained as the sum over all individual site–site interactions,

$$V(R, \theta_1, \theta_2, \phi) = \sum_{i=1}^{7} \sum_{j=1}^{5} V_{ij}\left[R_{ij}(R, \theta_1, \theta_2, \phi)\right]. \tag{4}$$

To remain consistent with the potential functions of Hellmann[5,6] for the like-species interactions and to allow for easy implementation into computer codes, the site positions and site charges of the two molecules were chosen to be identical to those of the interaction potentials of the pure components. The site positions are visualized in Fig. 1(b). Due to symmetry, there are only four distinct types of sites

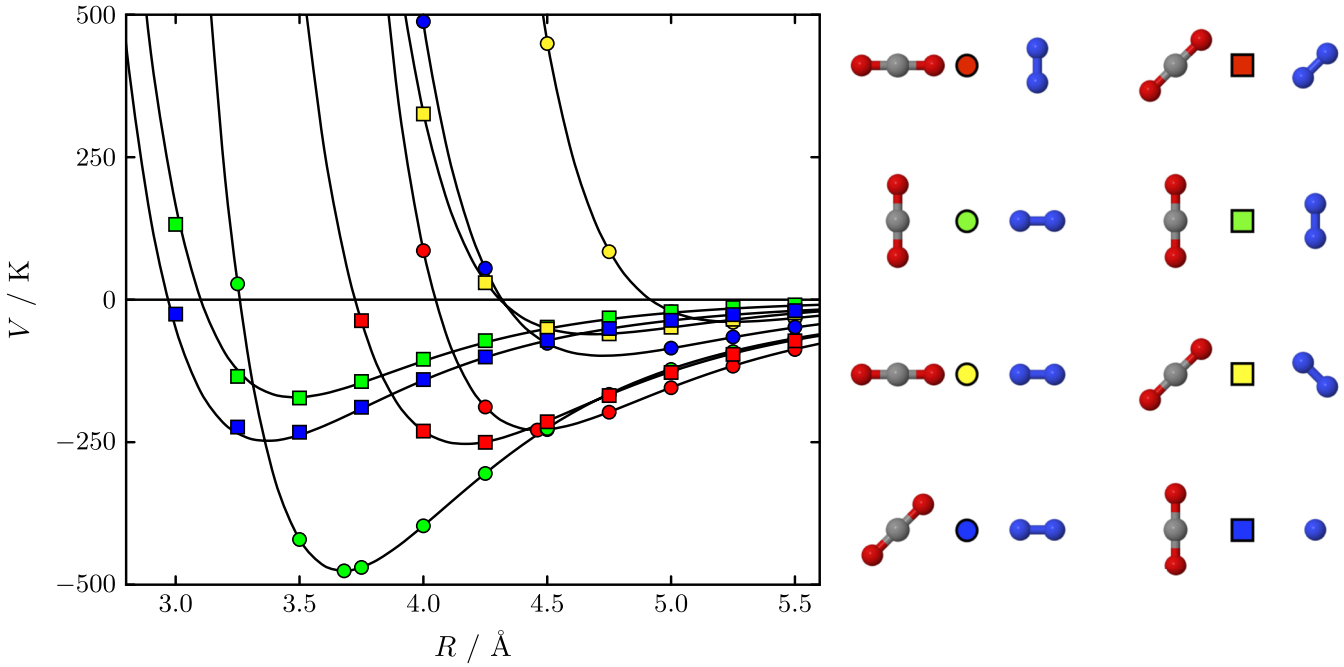

FIG. 2. CO_2—N_2 pair potential as a function of the center-of-mass distance R for 8 of the 93 considered angular configurations. The *ab initio* calculated values are represented by symbols, and the fitted analytical potential function is represented by solid lines. The orientations of the two minima of the PES correspond to the T-shaped configurations.

in CO_2 and three in N_2. The parameters A, α, b, and C_6 for the resulting 12 types of site–site interactions were optimized in a non-linear least-squares fit to the 1891 *ab initio* interaction energies. The C_6 parameters were constrained to give an isotropic average of the C_6 dispersion coefficient for CO_2—N_2, $C_{6\,\mathrm{iso}} = \sum_{i=1}^{7}\sum_{j=1}^{5} C_{6\,ij}$, equal to the accurate value of 107.9 a.u. obtained by Jhanwar and Meath[33] from the dipole oscillator strength distribution (DOSD). Initially, an exploratory fit of the PES was performed. The two minimum configurations of that exploratory potential function were then identified, and quantum-chemical calculations were performed for these two configurations in the same manner as for the other 1891 points before. Assuming these configurations to be close to the true minima of the PES, they served to refine the final fit of the potential function, now based on a total of 1893 points. During the fit, all values were weighted by

$$w = \frac{\exp\left[0.005\left(R/\text{Å}\right)^3\right]}{\left[1 + 10^{-6}(V/\text{K} + 500)^2\right]^2}. \tag{5}$$

The denominator of this function ensures that the weight of configurations increases with the interaction energy decreasing toward its most negative values ($V > -500$ K for all calculated interaction energies), whereas the numerator ensures an adequate fit quality at large R values, which is of particular importance for the calculation of the second virial coefficient. Similar weighting functions were already employed by Hellmann in previous studies.[8,9,17] An additional weight factor of 100 was used for the energies of both minimum configurations to ensure a perfect match.

Figure 2 shows the distance dependence of the *ab initio* interaction energies and of the fitted analytical potential function for 8 of the 93 considered angular configurations. In Fig. 3, the fitted interaction energies are plotted against the corresponding *ab initio* values for energies up to 50 000 K. The deviations from a straight line are very small, demonstrating the high quality of the fit. We calculated the mean absolute error (MAE) of the fit to be 1.04 K for negative interaction energies, 6.36 K for positive ones up to 2000 K, and 29.4 K between 2000 K and 10 000 K. The MAE increases even further in the

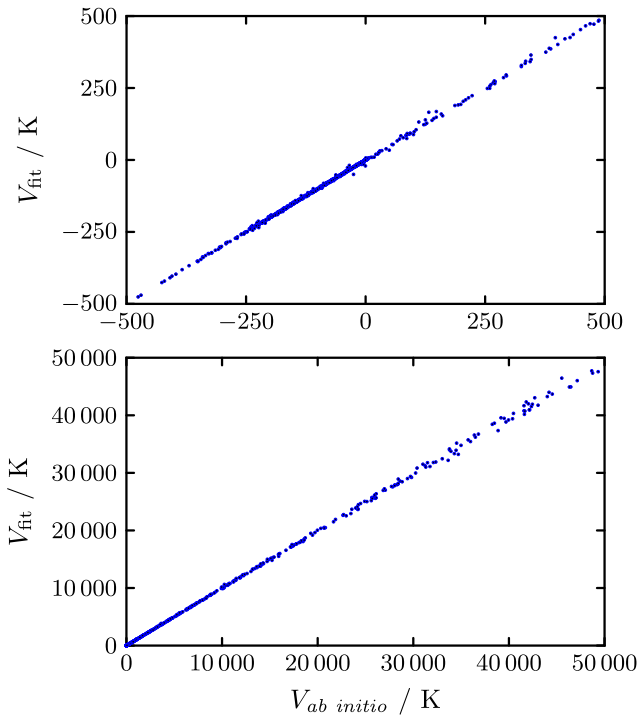

FIG. 3. Interaction energies from the fitted analytical potential function *versus* the corresponding *ab initio* values.

TABLE I. Comparison of the two minima of the present PES for the CO_2—N_2 molecule pair with the minima identified by Nasri *et al.* (Ref. 18).

	$\theta_1 = 90°, \theta_2 = 0°$		$\theta_1 = 0°, \theta_2 = 90°$	
	R (Å)	V (K)	R (Å)	V (K)
Reference 18, relaxed	3.683	−467.65	4.456	−229.66
Reference 18, rigid	3.694	−462.19	4.482	−228.62
This work, rigid	3.677	−475.76	4.460	−228.77

interval between 10 000 K and the highest interaction energies of almost 200 000 K. However, these interaction energies are of very little importance unless dealing with applications at extremely high temperatures.

The two symmetry-distinct minima of the analytical PES resemble perfect T-shaped angular orientations (both shown in Fig. 2) with interaction energies of −228.77 K ($\theta_1 = 0°$, $\theta_2 = 90°$) and −475.76 K ($\theta_1 = 90°$, $\theta_2 = 0°$). This is in agreement with the findings of Nasri *et al.*,[18] who performed supermolecular CCSD(T)-F12a[34]/aug-cc-pVTZ calculations, both for the case that all degrees of freedom are relaxed and for the case that rigid equilibrium structures of the two monomers are used to identify the two minima. Since we used zero-point vibrationally averaged monomer geometries in the present work, small differences when comparing the results are to be expected. The minimum distances and their respective energy values are given in Table I.

The parameters of the new analytical PES and a Fortran 90 routine that evaluates it are given in the supplementary material.

III. CROSS SECOND VIRIAL COEFFICIENT

For rigid molecules, the classical expression for the cross second virial coefficient as a function of temperature is

$$B_{12}^{\mathrm{cl}} = -\frac{N_{\mathrm{A}}}{2}\int_0^\infty \langle f_{12}\rangle_{\Omega_1,\Omega_2} d\mathbf{R}, \tag{6}$$

with

$$f_{12} = \exp\left[-\frac{V(\mathbf{R},\Omega_1,\Omega_2)}{k_{\mathrm{B}}T}\right] - 1. \tag{7}$$

Here, $\mathbf{R}$ is the distance vector between the centers of mass of the two molecules, Ω_1 and Ω_2 represent the angular orientations of molecules 1 and 2, respectively, and the angle brackets denote an average over Ω_1 and Ω_2. To account for quantum effects, the intermolecular pair potential V in Eq. (7) was replaced by the quadratic Feynman–Hibbs (QFH) effective pair potential,[35] which, for the CO_2—N_2 molecule pair, can be written as

$$V_{\mathrm{QFH}} = V + \frac{\hbar^2}{24k_{\mathrm{B}}T}\left[\frac{1}{\mu}\left(\frac{\partial^2 V}{\partial x^2} + \frac{\partial^2 V}{\partial y^2} + \frac{\partial^2 V}{\partial z^2}\right) + \frac{1}{I_1}\left(\frac{\partial^2 V}{\partial \psi_{1,a}^2} + \frac{\partial^2 V}{\partial \psi_{1,b}^2}\right) + \frac{1}{I_2}\left(\frac{\partial^2 V}{\partial \psi_{2,a}^2} + \frac{\partial^2 V}{\partial \psi_{2,b}^2}\right)\right], \tag{8}$$

where μ denotes the reduced mass of the molecule pair, x, y, and z are the Cartesian components of $\mathbf{R}$, I_i is the moment of inertia of molecule i, and the angles $\psi_{i,a}$ and $\psi_{i,b}$ correspond to rotations around the principal axes of molecule i.

The Mayer-sampling Monte Carlo (MSMC) approach of Singh and Kofke[36] was employed to compute the cross second virial coefficient at 187 temperatures between 100 K and 2000 K using the hard-sphere fluid with σ = 4.5 Å as the reference system. The results for all temperatures were obtained simultaneously in multi-temperature simulations[5,36,37] with a sampling temperature of 100 K and 5×10^{10} trial moves. In each MC trial move, one of the molecules was rotated and displaced. The maximum step sizes for the MC moves were adjusted initially in short equilibration periods to achieve acceptance rates of 50%. All derivatives of the pair potential in Eq. (8) were evaluated analytically. Computed values for the virial coefficient from 16 independent simulation runs were averaged. The precision of the final results is better than 0.004 cm^3/mol at all temperatures.

Figure 4 shows the results for the cross second virial coefficient compared with experimental data from the literature[38–50] and with the correlation of Dymond *et al.*[51] The figure also displays our estimate of the combined standard uncertainty (i.e., coverage factor k = 1). We based this estimate on the difference in the values for the cross second virial coefficient resulting from using the proposed PES and a PES that we fitted to the interaction energies resulting from the highest computed levels of theory, but without extrapolation of the two correlation energy contributions to the CBS limit. The values obtained using the non-extrapolated PES have been used to define the upper uncertainty bound and have then been mirrored to give the lower uncertainty bound. With increasing temperature, this uncertainty estimate becomes increasingly smaller, and we recommend a minimum uncertainty of 0.5 cm^3/mol. Hence, we have

$$u(B_{12}^{\mathrm{QFH}}) = \max\left(\left|B_{12,\mathrm{CBS}}^{\mathrm{QFH}} - B_{12,\mathrm{non\text{-}extr.}}^{\mathrm{QFH}}\right|, 0.5\ \mathrm{cm}^3/\mathrm{mol}\right). \tag{9}$$

Brugge *et al.*[48] derived very accurate data for the cross second virial coefficient from isothermal pVT measurements using a Burnett apparatus, which are in close agreement with our *ab initio* calculated values. We note that we have reanalyzed the measurements of Martin *et al.*[46] using the more accurate values provided by Hellmann[5,6] for the pure-component virial coefficients, leading to excellent agreement. Several other data sets[39,40,47,50] agree within our stated uncertainty. However, the few available experimental data below ambient temperature often lie significantly outside our uncertainty interval, in particular, the data of Brewer,[43] of Ng,[44] and, at very low temperatures, of Yakimenko *et al.*[45] At ambient and higher temperatures, the data of Cottrell *et al.*[41] and the datum of Edwards and Roseveare[38] deviate quite strongly not only from our calculated values but from the consensus of other experimental data as well.

Figure 4 also shows the results for the classical cross second virial coefficient. The deviations from the semiclassical values obtained with the QFH effective pair potential decrease rapidly with temperature from −15.09 cm^3/mol at 100 K to only −0.02 cm^3/mol at 2000 K.

The electronic supplementary material lists both the classically calculated values (B_{12}^{cl}) and the semiclassically calculated ones (B_{12}^{QFH}). The uncertainties $u(B_{12}^{\mathrm{QFH}})$ are also given therein.

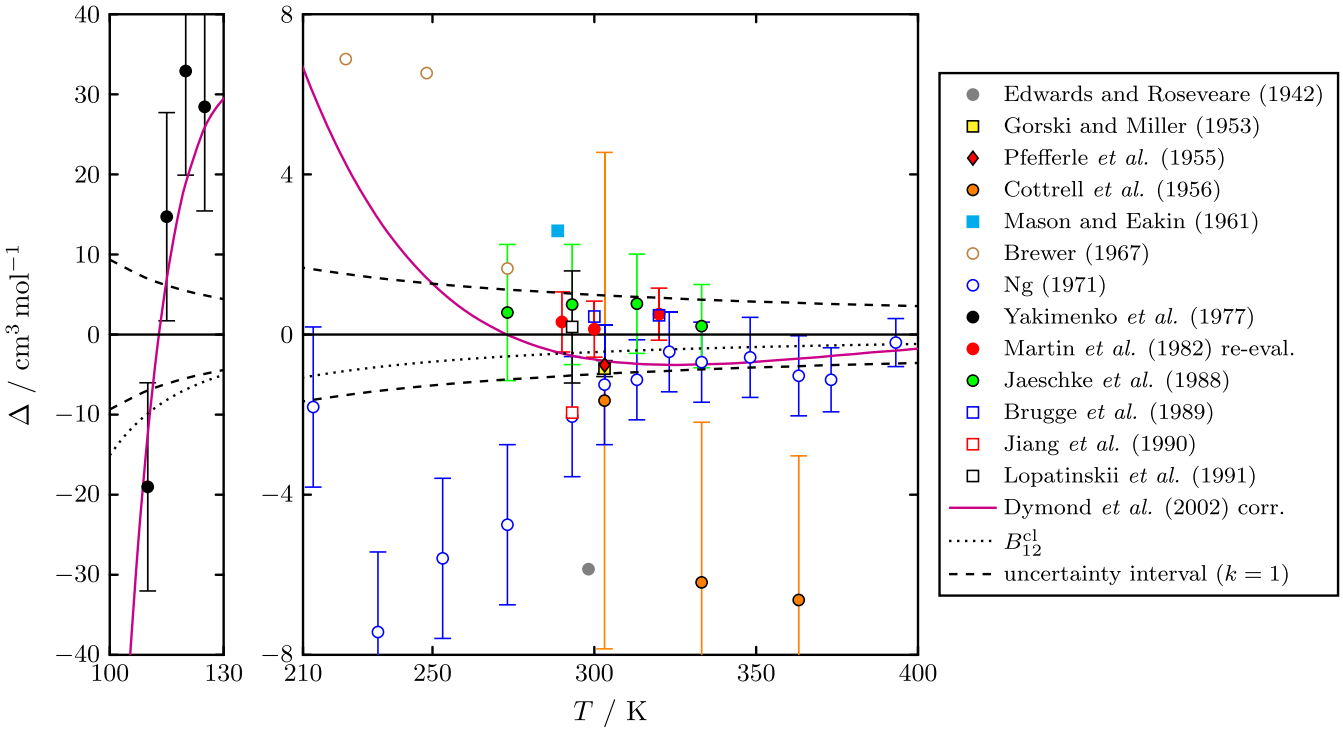

FIG. 4. Deviations, $\Delta = B_{12} - B_{12,}^{QFH}$, of experimental data,[38–50] the correlation of Dymond *et al.*,[51] and results from the classical statistical treatment (B_{12}^{cl}) for the CO_2—N_2 cross second virial coefficient from values obtained with Eq. (10). Both the data and the uncertainties of Ng[44] are as given by Dymond *et al.*[51]

An analytical expression for the cross second virial coefficient was found by fitting a polynomial in $(T^*)^{-1/2}$ with $T^* = T/(100\ \mathrm{K})$ to the 187 values for B_{12}^{QFH}. The structure of the polynomial was optimized using the symbolic regression software Eureqa (version 1.24.0).[52] The resulting expression,

$$\frac{B_{12}^{QFH}}{\mathrm{cm^3/mol}} = 24.025 + 128.09\,(T^*)^{-0.5} - 400.27\,(T^*)^{-1} - 303.38\,(T^*)^{-3.5} + 150.02\,(T^*)^{-4.5} - 71.935\,(T^*)^{-6}, \quad (10)$$

reproduces the calculated values within ±0.026 cm^3/mol.

IV. TRANSPORT PROPERTIES

A. Theory and computational details

The transport properties of a dilute gas mixture can be determined using the kinetic theory of molecular gases.[14–16,53–60] Each transport property is obtained by solving a system of linear equations, the coefficients of which are related to so-called generalized cross sections. The generalized cross sections are determined by the binary collisions of two molecules, which thus connects them directly to the intermolecular PES. The approach employed to determine values for transport properties from the generalized cross sections in the present work is the same as in previous studies.[14–16] Therefore, we do not repeat it here. In this work, we present results for the shear viscosity η in the third-order approximation, for the thermal conductivity λ (under steady-state conditions, see Ref. 15 for details) in the second-order approximation, and for the product of molar density and binary diffusion coefficient, $\rho_m D$, in the third-order approximation. Note that $\rho_m D$ is almost independent of composition and determined almost entirely by the unlike interaction, i.e., the CO_2—N_2 PES.

The determination of values for the thermal conductivity requires knowledge of the vibrational contributions to the ideal gas heat capacities of the pure gases, which were obtained from the current reference correlations[61,62] by subtracting the translational and classical rotational contributions. Hellmann used the same correlations in his studies on pure CO_2[6] and pure N_2.[5]

The generalized cross sections for binary collisions between CO_2 and N_2 were determined within the rigid-rotor approximation by means of the proven classical trajectory method using a modified version of the TRAJECT computer code.[59] The collision trajectories were obtained by integrating Hamilton's equations from pre- to postcollisional values. To avoid any cutoff effects, we used a very large initial and final separation of 500 Å. Total-energy-dependent generalized cross sections in the center-of-mass frame, which are 9-dimensional integrals over the initial states of the trajectories, were calculated by means of a simple Monte Carlo integration scheme using quasi-random numbers. The computations were performed for 33 values of the total energy, $E = E_{tr} + E_{rot}$, divided into the three ranges 60 K ⩽ E ⩽ 300 K, 300 K ⩽ E ⩽ 3000 K, and 3000 K ⩽ E ⩽ 60 000 K. In each range, the energies were chosen as the pivot points for Chebyshev interpolation of the cross sections as a function of ln(E); the cross sections are smooth functions

of energy. Up to 8×10^6 trajectories were calculated at each total energy value. Below 300 K, the number of trajectories was gradually reduced down to 800 000 at 60 K because of the increasing computational cost of calculating trajectories with the desired accuracy at lower energies. A weighted integration over the total energy yielded temperature-dependent generalized cross sections in the center-of-mass frame at temperatures from 150 K to 2000 K. The center-of-mass cross sections were then converted to the laboratory frame cross sections needed to determine the transport properties.

The generalized cross sections for the pure species collisions, i.e., those between two CO_2 and between two N_2 molecules, were obtained in a similar manner, the details of which have been published previously.[6,14]

B. Results and discussion

The values obtained for the shear viscosity, the thermal conductivity, and the binary diffusion coefficient of dilute gas mixtures of CO_2 and N_2 are provided at 173 temperatures from 150 K to 2000 K and for 11 mole fractions in the supplementary material. The variation of the product of molar density and binary diffusion coefficient with mole fraction does not exceed 0.45% at any temperature. We estimate the precision of the computed transport property values to be better than 0.1% for shear viscosity and diffusion and better than 0.2% for thermal conductivity. These values are based on precision estimates generated by TRAJECT for the individual generalized cross sections; see Ref. 63 for details.

We recommend a small scaling of the calculated viscosity values (as suggested by Hellmann for CO_2[6] and by Hellmann *et al.* for N_2[14]), which is based on highly accurate measurements of Vogel[64,65] for the two pure substances. Assuming a simple linear dependence of the correction on the mole fraction, we have

$$\eta = \eta_{\mathrm{cal}}(1.0055\, x_{\mathrm{CO_2}} + 1.0024\, x_{\mathrm{N_2}}), \tag{11}$$

where the scaling factors 1.0055 and 1.0024 correspond to those given in Refs. 6 and 14. The computed values for viscosity as well as the scaled ones are compared in Fig. 5 against the available experimental data.[64–70] The best experimental data are those of Kestin and co-workers[66,67,69] close to room temperature and the recently reported data of Humberg *et al.*,[70] which lie mostly within ±0.25% of our proposed scaled viscosity values. The high-temperature data ($T > 298$ K) of Kestin and Ro are known to suffer from a design flaw[71] in their viscometer that resulted in viscosity values that are always systematically too high above room temperature by up to about 1%.[5,10,13,14,16,17,65] This is consistent with the observed deviations.

We conservatively estimate the combined standard uncertainty of the scaled values to vary from 0.2% for pure CO_2 to 0.15% for pure N_2 between 300 K and 700 K, increasing to 1% for pure CO_2 and 0.5% for pure N_2, respectively, outside of this temperature range.

We also propose a scaling of the calculated thermal conductivity values,

$$\lambda = \lambda_{\mathrm{cal}}(1.011\, x_{\mathrm{CO_2}} + x_{\mathrm{N_2}}), \tag{12}$$

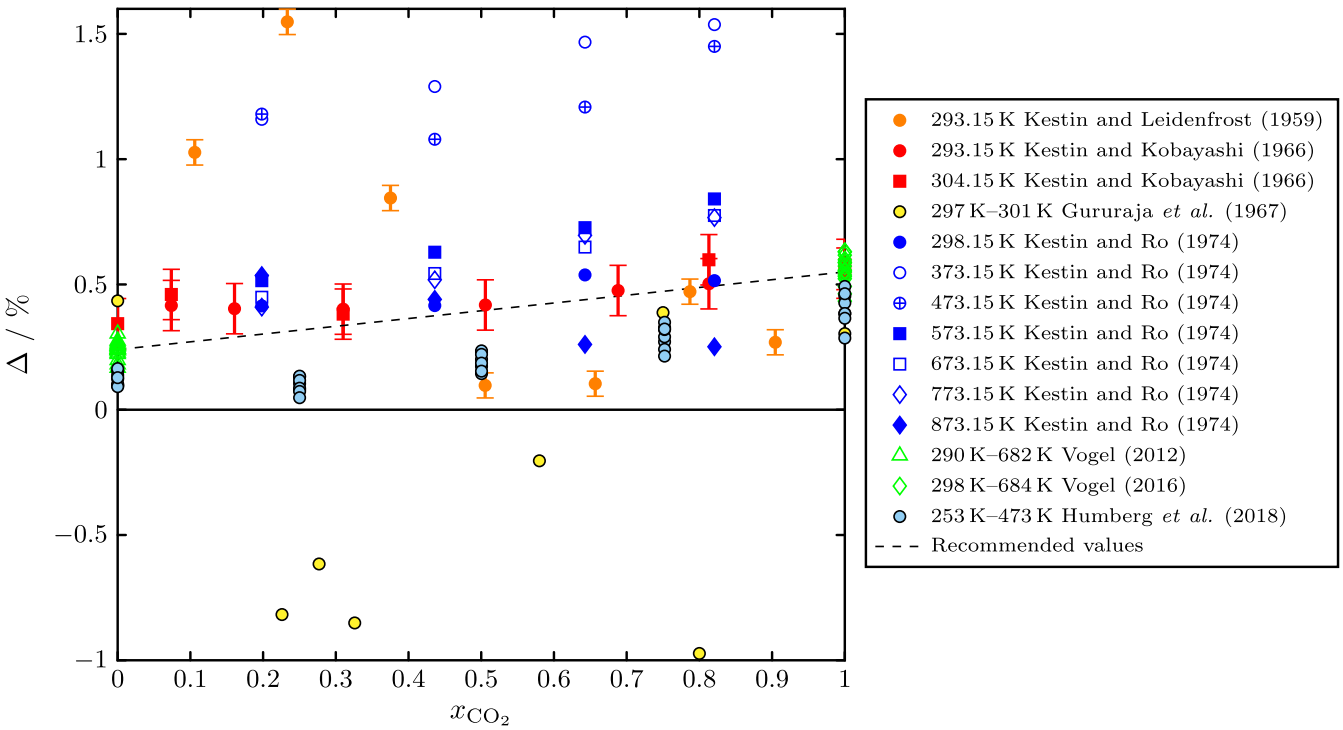

FIG. 5. Deviations, $\Delta = (\eta_{\mathrm{exp}} - \eta_{\mathrm{cal}})/\eta_{\mathrm{cal}}$, of experimental viscosity data[64–70] for dilute CO_2–N_2 mixtures and the pure components from the calculated values. For clarity of the figure, the stated uncertainties for the data of Kestin and Ro[69] (<0.3%), Vogel[64,65] (<0.4%), and Humberg *et al.*[70] (<0.4%) are not indicated by error bars. The dashed line indicates the recommended values given by Eq. (11).

with the scaling parameter 1.011 recommended by Hellmann[6] based on the comparison with the accurate measurements by Haarman[72] for pure CO_2. The combined standard uncertainty for the scaled values is estimated to vary from 1% for pure CO_2 to 0.5% for pure N_2 between 300 K and 700 K, increasing to 2% for pure CO_2 and 1% for pure N_2 outside of this temperature range. Figure 6 compares the available experimental data from the literature with our calculated and proposed scaled values. We observe that the available experimental data[73–79] exhibit a large scatter, which is not possible to reconcile with the claimed uncertainties of different workers. In light of the experimental data situation and proven track record of results obtained from kinetic theory in conjunction with accurate *ab initio* potentials, it is safe to say that the proposed scaled values can be considered the most accurate available data for the thermal conductivity of low-density gas mixtures of carbon dioxide and nitrogen.

The results for the binary diffusion coefficient are compared with several experimental data sets[80–92] in Fig. 7. Our results are corroborated particularly by the data of Robjohns and Dunlop[92] (provided in the form of a smoothing function). The agreement is within ±0.2% over the whole temperature range (277 K to 323 K) of the experimental data. Binary diffusion coefficients measured by the Dunlop group are consistently in excellent agreement with theoretically calculated values, as illustrated for other dilute gas systems.[17,93] The other experimental data shown in Fig. 7 exhibit larger scatter and have larger uncertainties than that of Robjohns and Dunlop, especially the high-temperature data of Pakurar and Ferron, which have quoted uncertainties of 10%. Nevertheless, they do generally support the temperature trend of our calculated values. We conservatively estimate the combined standard uncertainties of our calculated values to be 1% between 300 K and 700 K and 1.5% below 300 K and above 700 K. Finally, for completeness, we have also evaluated the parameter A^* that appears in kinetic theory and is proportional to the ratio of the binary diffusion coefficient and the interaction viscosity.[14,58] It is a function of the unlike interaction only, and for the CO_2—N_2 system, it exhibits the typical behavior already observed for other polyatomic gases.[8,94] It increases with temperature from 1.136 at 150 K to 1.160 at 200 K and then remains relatively constant, reaching a value of 1.180 at 2000 K.

C. Correlation for the binary diffusion coefficient

We have developed a correlation for the binary diffusion coefficient of the CO_2—N_2 system in the dilute gas limit based on the calculated values of the present work. For ease of use, we neglected the very small composition dependence and fitted the correlation to the values for an equimolar mixture. The correlation is of the form

$$\frac{10^4 \times \rho_m D}{\text{mol m}^{-1}\,\text{s}^{-1}} = \frac{\overline{T}^{1/2}}{S(\overline{T})}, \tag{13}$$

where $\overline{T} = T/\text{K}$ and $S(\overline{T})$ is a function that would be proportional to a single generalized cross section if $\rho_m D$ were to be

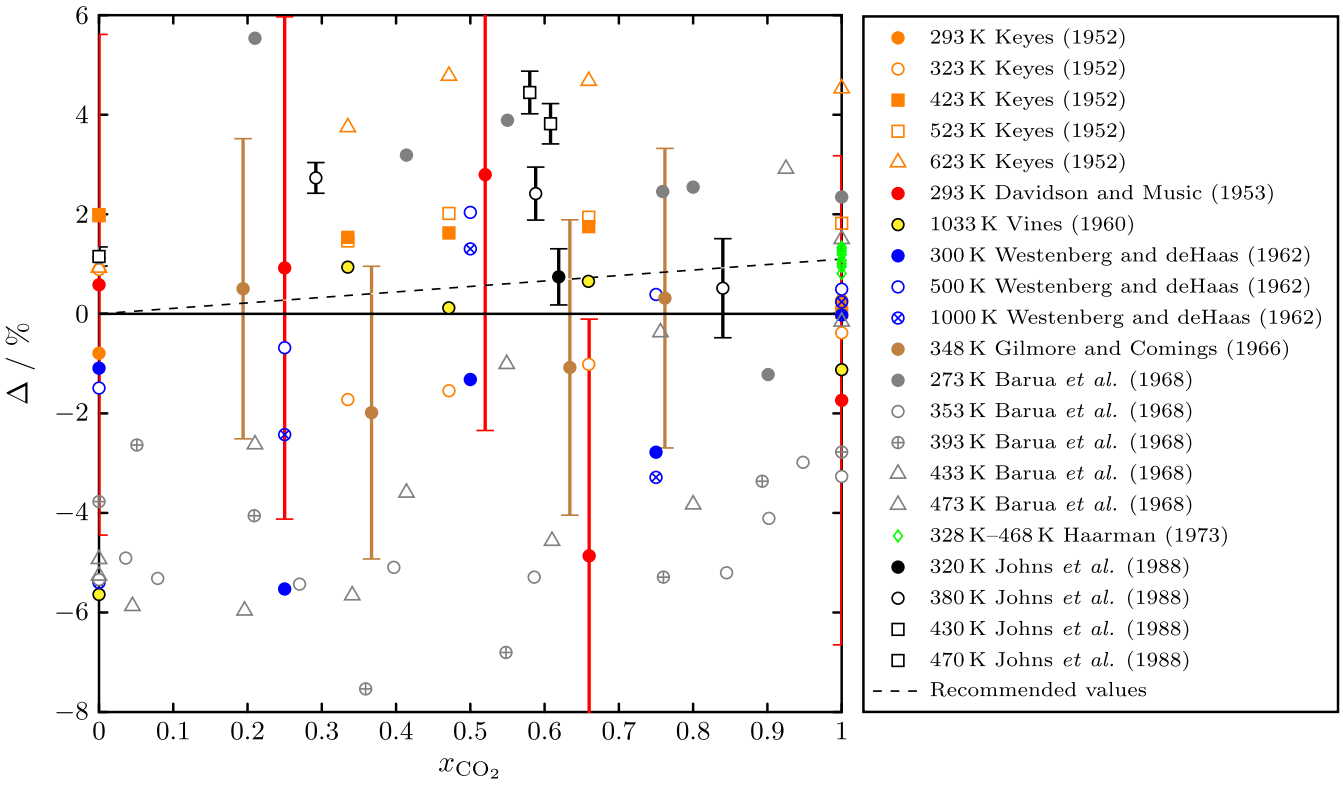

FIG. 6. Deviations, $\Delta = (\lambda_{exp} - \lambda_{cal})/\lambda_{cal}$, of experimental thermal conductivity data[72–79] for dilute CO_2—N_2 mixtures and the pure components from the calculated values. For clarity of the figure, the stated uncertainties for the data of Barua *et al.*[78] (1% for the pure gases and 2% for the mixtures) and Haarman[72] (0.3%) are not indicated by error bars. The dashed line indicates the recommended values given by Eq. (12).

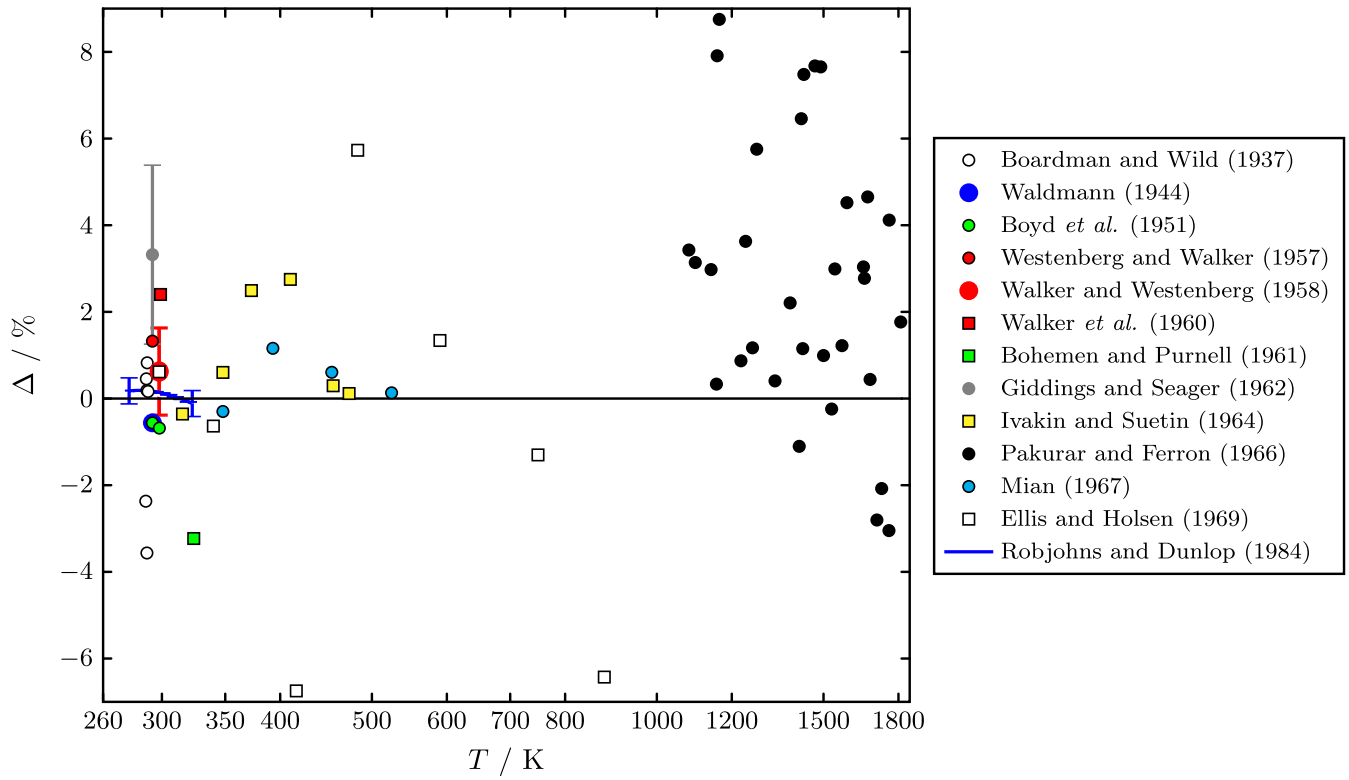

FIG. 7. Deviations, $\Delta = (\rho_m D_{exp} - \rho_m D_{cal})/\rho_m D_{cal}$, of experimental values[80–92] for the binary diffusion coefficient of a dilute CO_2—N_2 mixture from the calculated values. For clarity of the figure, the stated uncertainty for the data of Pakurar and Ferron[89] (10%) is not indicated by error bars.

obtained from the first-order kinetic theory. This generalized cross section is known to decrease monotonically with temperature and, for rigid molecules, to approach a constant value at very high temperatures (hard-sphere behavior). To find a functional form for $S(\overline{T})$ that obeys these constraints, while being both simple and accurate, we used again the symbolic regression software Eureqa. Hellmann correlated the self-diffusion coefficient of ethane in a similar way.[8] He allowed $\overline{T}$ to appear solely in integer powers of $\overline{T}^{1/6}$. In addition, only constants, exponential functions, and the operators addition, subtraction, multiplication, division, and negation were allowed to occur. Following this approach, we obtained a three-parameter function that fulfills all requirements,

$$S(\overline{T}) = 0.102\,61 + 5.5239\,\overline{T}^{-1/6} + 94.161\,\overline{T}^{1/6}\exp\left(-\overline{T}^{1/3}\right). \tag{14}$$

The correlation reproduces the calculated values within ±0.1%. Its uncertainty corresponds approximately to that of the calculated values (see above). Figure 8 shows that the correlation extrapolates in a physically reasonable manner down to zero kelvin and up to several thousand kelvin.

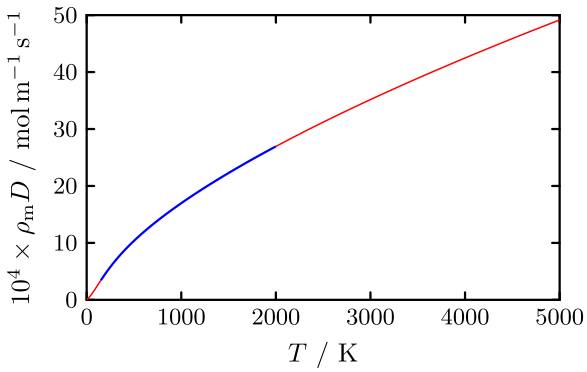

FIG. 8. Correlation for the product of the molar density and the binary diffusion coefficient of dilute CO_2—N_2 gas mixtures as given by Eqs. (13) and (14). The correlation is colored in blue within its range of validity and in red outside of this range.

V. SUMMARY AND CONCLUSIONS

A new intermolecular PES for the CO_2—N_2 molecule pair was determined from counterpoise-corrected supermolecular *ab initio* calculations at the RI-MP2 and CCSD(T) levels of theory with basis sets of up to quintuple-zeta quality and quadruple-zeta quality, respectively. In total, interaction energies for 1893 distinct geometries of the molecule pair were computed and extrapolated to the CBS limit. An analytical site–site potential function with seven sites for the CO_2 molecule and five sites for the N_2 molecule was fitted to the interaction energies. The PES exhibits two distinct minima, corresponding to the two possible T-shaped configurations, with interaction energies of −228.77 K and −475.76 K.

The analytical PES was used to calculate the CO_2—N_2 cross second virial coefficient using classical statistical mechanics in conjunction with an effective pair potential following Feynman and Hibbs[35] to account for quantum effects. The respective integral expression was solved numerically by means of the MSMC method.[36] The comparison with the best

available experimental data shows a highly satisfactory level of agreement.

Furthermore, we determined transport properties of the CO_2—N_2 system at low gas densities in the temperature range from 150 K to 2000 K using the classical trajectory method in conjunction with the kinetic theory of molecular gases.[53–60] The new PES was used to calculate the required generalized cross sections for the collisions of a CO_2 molecule with an N_2 molecule, while the generalized cross sections for the like-species interactions were taken from prior studies.[6,14] Based on the comparison with the best available experimental data for the pure gases, we propose a small correction to our calculated values for both shear viscosity and thermal conductivity using a temperature-independent scaling factor. We provide error estimates for our proposed transport property values, which, depending on the property, temperature, and mole fraction, range from 0.15% to 2%. All calculated values for the cross second virial coefficient and the three transport properties are listed in the supplementary material.

For the cross second virial coefficient and the binary diffusion coefficient, we also developed simple but accurate correlations, which are based entirely on our calculated values. The very small composition dependence of the binary diffusion coefficient is neglected in the correlation.

In conclusion, the newly developed PES for the CO_2—N_2 molecule pair has been successfully validated by the comparison of the resulting thermophysical property values with the best available experimental data. Given the lack of reliable and accurate thermophysical property data in a wide range of composition and temperature, especially for the thermal conductivity and the binary diffusion coefficient, the current calculated values constitute a reliable and accurate set of thermophysical property data valid for all CO_2—N_2 mixture compositions and temperatures as low as 150 K and as high as 2000 K.

SUPPLEMENTARY MATERIAL

See supplementary material for the details of the internal coordinates of the CO_2—N_2 system, the results of the *ab initio* calculations for the 1893 investigated PES points, a Fortran 90 routine computing the analytical potential function, and tables of the thermophysical property values calculated in this work.

ACKNOWLEDGMENTS

J.C.C.-P. and V.V. acknowledge financial support by the Imperial College Trust.

[1] R. Hellmann, E. Bich, and E. Vogel, J. Chem. Phys. **128**, 214303 (2008).
[2] R. Bukowski, K. Szalewicz, G. C. Groenenboom, and A. van der Avoird, J. Chem. Phys. **128**, 094313 (2008).
[3] K. Patkowski, W. Cencek, P. Jankowski, K. Szalewicz, J. B. Mehl, G. Garberoglio, and A. H. Harvey, J. Chem. Phys. **129**, 094304 (2008).
[4] R. Hellmann, E. Bich, E. Vogel, and V. Vesovic, Phys. Chem. Chem. Phys. **13**, 13749 (2011).
[5] R. Hellmann, Mol. Phys. **111**, 387 (2013).
[6] R. Hellmann, Chem. Phys. Lett. **613**, 133 (2014).
[7] J.-P. Crusius, R. Hellmann, E. Hassel, and E. Bich, J. Chem. Phys. **141**, 164322 (2014).
[8] R. Hellmann, J. Chem. Eng. Data **63**, 470 (2018).
[9] R. Hellmann, J. Chem. Phys. **146**, 114304 (2017).
[10] R. Hellmann, E. Bich, E. Vogel, A. S. Dickinson, and V. Vesovic, J. Chem. Phys. **129**, 064302 (2008).
[11] R. Hellmann, E. Bich, E. Vogel, A. S. Dickinson, and V. Vesovic, J. Chem. Phys. **130**, 124309 (2009).
[12] R. Hellmann and E. Bich, Mol. Phys. **113**, 176 (2015).
[13] R. Hellmann and E. Vogel, J. Chem. Eng. Data **60**, 3600 (2015).
[14] R. Hellmann, E. Bich, E. Vogel, and V. Vesovic, J. Chem. Phys. **141**, 224301 (2014).
[15] R. Hellmann, E. Bich, and V. Vesovic, J. Chem. Phys. **144**, 134301 (2016).
[16] R. Hellmann, E. Bich, and V. Vesovic, J. Chem. Thermodyn. **102**, 429 (2016).
[17] R. Hellmann, J. Chem. Eng. Data **63**, 246 (2018).
[18] S. Nasri, Y. Ajili, N.-E. Jaidane, Y. N. Kalugina, P. Halvick, T. Stoecklin, and M. Hochlaf, J. Chem. Phys. **142**, 174301 (2015).
[19] K. Raghavachari, G. W. Trucks, J. A. Pople, and M. Head-Gordon, Chem. Phys. Lett. **157**, 479 (1989).
[20] S. F. Boys and F. Bernardi, Mol. Phys. **19**, 553 (1970).
[21] F. Weigend and M. Häser, Theor. Chem. Acc. **97**, 331 (1997).
[22] F. Weigend, M. Häser, H. Patzelt, and R. Ahlrichs, Chem. Phys. Lett. **294**, 143 (1998).
[23] F. Weigend, M. Kattannek, and R. Ahlrichs, J. Chem. Phys. **130**, 164106 (2009).
[24] S. Kossmann and F. Neese, Chem. Phys. Lett. **481**, 240 (2009).
[25] R. A. Kendall, T. H. Dunning, Jr., and R. J. Harrison, J. Chem. Phys. **96**, 6796 (1992).
[26] F. Weigend, Phys. Chem. Chem. Phys. **4**, 4285 (2002).
[27] F. Weigend, A. Köhn, and C. Hättig, J. Chem. Phys. **116**, 3175 (2002).
[28] K. Patkowski, J. Chem. Phys. **138**, 154101 (2013).
[29] A. Halkier, T. Helgaker, P. Jørgensen, W. Klopper, H. Koch, J. Olsen, and A. K. Wilson, Chem. Phys. Lett. **286**, 243 (1998).
[30] F. Neese, Wiley Interdiscip. Rev.: Comput. Mol. Sci. **2**, 73 (2012).
[31] CFOUR, Coupled-Cluster techniques for Computational Chemistry, a quantum-chemical program package by J. F. Stanton, J. Gauss, M. E. Harding, and P. G. Szalay with contributions from A. A. Auer, R. J. Bartlett, U. Benedikt, C. Berger, D. E. Bernholdt, Y. J. Bomble, L. Cheng, O. Christiansen, M. Heckert, O. Heun, C. Huber, T.-C. Jagau, D. Jonsson, J. Jusélius, K. Klein, W. J. Lauderdale, D. A. Matthews, T. Metzroth, L. A. Mück, D. P. O'Neill, D. R. Price, E. Prochnow, C. Puzzarini, K. Ruud, F. Schiffmann, W. Schwalbach, S. Stopkowicz, A. Tajti, J. Vázquez, F. Wang, and J. D. Watts, and the integral packages MOLECULE (J. Almlöf and P. R. Taylor), PROPS (P. R. Taylor), ABACUS (T. Helgaker, H. J. Aa. Jensen, P. Jørgensen, and J. Olsen), and ECP routines by A. V. Mitin and C. van Wüllen. For the current version, see http://www.cfour.de.
[32] K. T. Tang and J. P. Toennies, J. Chem. Phys. **80**, 3726 (1984).
[33] B. L. Jhanwar and W. J. Meath, Chem. Phys. **67**, 185 (1982).
[34] T. B. Adler, G. Knizia, and H.-J. Werner, J. Chem. Phys. **127**, 221106 (2007).
[35] R. P. Feynman and A. R. Hibbs, *Quantum Mechanics and Path Integrals* (McGraw-Hill, New York, 1965).
[36] J. K. Singh and D. A. Kofke, Phys. Rev. Lett. **92**, 220601 (2004).
[37] B. Jäger, R. Hellmann, E. Bich, and E. Vogel, J. Chem. Phys. **135**, 084308 (2011).
[38] A. E. Edwards and W. E. Roseveare, J. Am. Chem. Soc. **64**, 2816 (1942).
[39] R. A. Gorski and J. G. Miller, J. Am. Chem. Soc. **75**, 550 (1953).
[40] W. C. Pfefferle, Jr., J. A. Goff, and J. G. Miller, J. Chem. Phys. **23**, 509 (1955).
[41] T. L. Cottrell, R. A. Hamilton, and R. P. Taubinger, Trans. Faraday Soc. **52**, 1310 (1956).
[42] D. M. Mason and B. E. Eakin, J. Chem. Eng. Data **6**, 499 (1961).
[43] J. Brewer, Technical Report No. 67–2795, AFOSR, 1967.
[44] H.-J. Ng, M.S. thesis, University of Alberta, Edmonton, Alberta, Canada, 1971.
[45] N. P. Yakimenko, G. M. Glukh, and M. B. Iomtev, Zh. Fiz. Khim. **51**, 1566 (1977).
[46] M. L. Martin, R. D. Trengove, K. R. Harris, and P. J. Dunlop, Aust. J. Chem. **35**, 1525 (1982).
[47] M. Jaeschke, S. Audibert, P. van Caneghem, A. E. Humphreys, R. Janssen-van Rosmalen, Q. Pellei, J. P. J. Michels, J. A. Schouten, and C. A. ten Seldam, *GERG Technical Monograph 2* (Verlag des Vereins Deutscher Ingenieure, Düsseldorf, 1988), p. 163.
[48] H. B. Brugge, C.-A. Hwang, W. J. Rogers, J. C. Holste, K. R. Hall, W. Lemming, G. J. Esper, K. N. Marsh, and B. E. Gammon, Physica A **156**, 382 (1989).

[49]S. Jiang, Y. Wang, and J. Shi, Fluid Phase Equilib. **57**, 105 (1990).
[50]E. S. Lopatinskiii, M. S. Rozhnov, V. I. Zhdanov, S. L. Parnovskii, and Y. N. Kudrya, Zh. Fiz. Khim. **65**, 2060 (1991).
[51]J. H. Dymond, K. N. Marsh, and R. C. Wilhoit, in *Landolt-Börnstein: Numerical Data and Functional Relationships in Science and Technology: New Series*, Group IV: Physical Chemistry: Virial Coefficients of Mixtures, edited by M. Frenkel and K. N. Marsh (Springer, Berlin–Heidelberg–New York, 2002), Vol. 21B, Chap. 2, pp. 80–82.
[52]M. Schmidt and H. Lipson, Science **324**, 81 (2009).
[53]L. Waldmann, "Transporterscheinungen in Gasen von mittlerem Druck," in *Handbuch der Physik*, edited by S. Flügge (Springer-Verlag, Berlin, 1958), Vol. 12, pp. 295–514.
[54]L. Waldmann and E. Trübenbacher, Z. Naturforsch. A **17**, 363 (1962).
[55]J. H. Ferziger and H. G. Kaper, *The Mathematical Theory of Transport Processes in Gases* (North-Holland, Amsterdam, 1972).
[56]C. F. Curtiss, J. Chem. Phys. **75**, 1341 (1981).
[57]M. Mustafa, "Measurement and calculation of transport properties of polyatomic gases," Ph.D. thesis, Imperial College London, London, UK, 1987.
[58]F. R. W. McCourt, J. J. M. Beenakker, W. E. Köhler, and I. Kuščer, *Nonequilibrium Phenomena in Polyatomic Gases*, Vol. I: Dilute Gases (Clarendon Press, Oxford, 1990).
[59]E. L. Heck and A. S. Dickinson, Comput. Phys. Commun. **95**, 190 (1996).
[60]A. S. Dickinson, R. Hellmann, E. Bich, and E. Vogel, Phys. Chem. Chem. Phys. **9**, 2836 (2007).
[61]R. Span and W. Wagner, J. Phys. Chem. Ref. Data **25**, 1509 (1996).
[62]R. Span, E. W. Lemmon, R. T. Jacobsen, W. Wagner, and A. Yokozeki, J. Phys. Chem. Ref. Data **29**, 1361 (2000).
[63]E. L. Heck and A. S. Dickinson, Mol. Phys. **81**, 1325 (1994).
[64]E. Vogel, Int. J. Thermophys. **33**, 741 (2012).
[65]E. Vogel, Int. J. Thermophys. **37**, 63 (2016).
[66]J. Kestin and W. Leidenfrost, Physica **25**, 525 (1959).
[67]J. Kestin, Y. Kobayashi, and R. T. Wood, Physica **32**, 1065 (1966).
[68]G. J. Gururaja, M. A. Tirunarayanan, and A. Ramachandran, J. Chem. Eng. Data **12**, 562 (1967).
[69]J. Kestin and S. T. Ro, Ber. Bunsenges. Phys. Chem. **78**, 20 (1974).
[70]K. Humberg, M. Richter, J. P. M. Trusler, and R. Span, J. Chem. Thermodyn. **120**, 191 (2018).
[71]E. Vogel, C. Küchenmeister, E. Bich, and A. Laesecke, J. Phys. Chem. Ref. Data **27**, 947 (1998).
[72]J. W. Haarman, AIP Conf. Proc. **11**, 193 (1973).
[73]F. G. Keyes, Trans. ASME **74**, 1303 (1952).
[74]J. M. Davidson and J. F. Music, Report HW-29021, Hanford Atomic Products Operation, Richland, WA, 1953.
[75]R. G. Vines, J. Heat Transfer **82**, 48 (1960).
[76]A. A. Westenberg and N. de Haas, Phys. Fluids **5**, 266 (1962).
[77]T. F. Gilmore and E. W. Comings, AIChE J. **12**, 1172 (1966).
[78]A. K. Barua, A. Manna, and P. Mukhopadhyay, J. Phys. Soc. Jpn. **25**, 862 (1968).
[79]A. I. Johns, S. Rashid, L. Rowan, J. T. R. Watson, and A. A. Clifford, Int. J. Thermophys. **9**, 3 (1988).
[80]L. E. Boardman and N. E. Wild, Proc. R. Soc. London, Ser. A **162**, 511 (1937).
[81]L. Waldmann, Naturwiss. **32**, 223 (1944).
[82]C. A. Boyd, N. Stein, V. Steingrimsson, and W. F. Rumpel, J. Chem. Phys. **19**, 548 (1951).
[83]A. A. Westenberg and R. E. Walker, J. Chem. Phys. **26**, 1753 (1957).
[84]R. E. Walker and A. A. Westenberg, J. Chem. Phys. **29**, 1139 (1958).
[85]R. E. Walker, N. deHaas, and A. A. Westenberg, J. Chem. Phys. **32**, 1314 (1960).
[86]J. Bohemen and J. H. Purnell, J. Chem. Soc. 360 (1961).
[87]J. C. Giddings and S. L. Seager, Ind. Eng. Chem. Fundam. **1**, 277 (1962).
[88]B. A. Ivakin and P. E. Suetin, Sov. Phys. Tech. Phys. **9**, 866 (1964).
[89]T. A. Pakurar and J. R. Ferron, Ind. Eng. Chem. Fundam. **5**, 553 (1966).
[90]A. A. Mian, "Measurement and prediction of binary gaseous diffusion coeffcients," Ph.D. thesis, Louisiana State University and Agricultural and Mechanical College, Baton Rouge, Louisiana, 1967.
[91]C. S. Ellis and J. N. Holsen, Ind. Eng. Chem. Fundam. **8**, 787 (1969).
[92]H. L. Robjohns and P. J. Dunlop, Ber. Bunsenges. Phys. Chem. **88**, 1239 (1984).
[93]B. Jäger and E. Bich, J. Chem. Phys. **146**, 214302 (2017).
[94]E. Bich, J. B. Mehl, R. Hellmann, and V. Vesovic, in *Experimental Thermodynamics Volume IX: Advances in Transport Properties of Fluids*, edited by M. J. Assael, A. R. H. Goodwin, V. Vesovic, and W. A. Wakeham (The Royal Society of Chemistry, Cambridge, 2014), Chap. 7, pp. 226–252.